HHS Public Access

Author manuscript

Curr Protoc Neurosci. Author manuscript; available in PMC 2018 April 10.

Published in final edited form as:

Curr Protoc Neurosci. ; 79: 1.28.1–1.28.24. doi:10.1002/cpns.28.

WGA-Alexa conjugates for axonal tracing

Sabrina L. Levy[1,4], **Joshua J. White**[1,2,4], **Elizabeth P. Lackey**[1,2,4], **Lindsey Schwartz**[1,2], and **Roy V. Sillitoe**[1,2,3,4,*]

[1]Department of Pathology & Immunology, 1250 Moursund Street, Suite 1325, Houston, Texas 77030, USA

[2]Department of Neurosciencem, 1250 Moursund Street, Suite 1325, Houston, Texas 77030, USA

[3]Program in Developmental Biology, 1250 Moursund Street, Suite 1325, Houston, Texas 77030, USA

[4]Baylor College of Medicine, Jan and Dan Duncan Neurological Research Institute of Texas Children's Hospital, 1250 Moursund Street, Suite 1325, Houston, Texas 77030, USA

Abstract

Anatomical labeling approaches are essential for understanding brain organization. Among these approaches are various methods of performing tract tracing. However, a major hurdle to overcome when marking neurons *in vivo* is visibility. Poor visibility makes it challenging to image a desired neuronal pathway so that it can be easily differentiated from a closely neighboring pathway. As a result, it becomes impossible to analyze individual projections or their connections. The tracer that is chosen for a given purpose has a major influence on the quality of the tracing. Here, we describe the wheat germ agglutinin (WGA) tracer conjugated to Alexa fluorophores for reliable high-resolution tracing of central nervous system projections. Using the mouse cerebellum as a model system, we implement WGA-Alexa tracing for marking and mapping neural circuits that control motor function. We also show its utility for marking localized regions of the cerebellum after performing single-unit extracellular recordings *in vivo*.

Keywords

WGA-Alexa; circuit tracing; connectivity; topography; cerebellum

INTRODUCTION

Many methods are now available for studying brain architecture. Among these are various approaches for labeling neurons *in vivo* (Zaborszky et al., 2010). In some cases, the method requires a current to deliver the specific marker and in other cases pressure injections are sufficient. Among the most extensively used tracing molecules are neurobiotin and biocytin, which are excellent for labeling single cells or phaseolus vulgaris leucoagglutinin (PHAL), labeled dextrans (fluoro-ruby and BDA), cholera toxin subunit B, lipophilic tracers (DiI, DiO, and DiA), viral tracers (herpes simplex and rabies virus), and wheat germ agglutinin

*Address correspondence to Dr. Roy V. Sillitoe, Tel: 832-824-8913, Fax: 832-825-1251, sillitoe@bcm.edu.

(WGA)-based tracers, which are all valuable for revealing synapses, circuits, and networks (Arenkiel, 2015). The tracer has to be actively or passively taken up by the cell and then transported via the axon into the soma and dendrite of that cell, or down the axon and transynaptically into a connected neuron. Regardless of what aspect of circuitry the tracer best reveals, in all cases the tracer molecule must be visible during imaging in order to fully appreciate the neuroanatomy that it reveals. However, other considerations must also be taken into account and include the speed of transport, flexibility to be paired with other histological methods, toxicity to the neural tissue, reliability to label different populations in distinct brain regions, and the ability to consistently target specific cells from animal to animal.

Here, we describe a circuit tracing approach that utilizes the WGA tracer conjugated to Alexa for examining brain projections. WGA is a lectin-based molecule. It is isolated from the wheat, Triticum vulgaris. In solution, WGA has a molecular weight of about 38kDa (Mesulam, 1982; Dumas et al., 1979b; Goldstein and Hayes, 1978; LeVine et al., 1972; Nicolson, 1974). It binds specifically to N-acetyl-D-glucosamine and N-acetylneuraminic acid (sialic acid) residues, which are ubiquitous in neuronal membranes (Mesulam, 1982). The specific affinity of WGA for neural membranes has made it one of the most extensively used tools for tracking neural connections in the brain, spinal cord, and peripheral nervous system (Borges and Sidman, 1982; van der Want et al., 1997). Moreover, because of its affinity for cellular membranes, it can travel in the anterograde and retrograde directions. However, once it is taken up by a neuron, it is not only transported bi-directionally, but in some cases it can even jump transganglionically (in peripheral circuits) or transynaptically (in central circuits) (Mesulam, 1982; Schwab et al., 1978; Dumas et al., 1979b; Coulter et al., 1980; Sillitoe, 2016). Moreover, it can be used by itself, or for some applications, its efficiency has been greatly enhanced after conjugating it to horseradish peroxide (HRP) (Staines et al., 1980; Sillitoe et al., 2010), or as we describe here, to fluorophores such as the Alexa dyes (Reeber et al., 2011a; Reeber et al., 2011b; Gebre et al., 2012; White et al., 2014).

In this study, we use the mouse cerebellum as a model system to demonstrate the utility of WGA-Alexa tracing for mapping neural projections *in vivo*. The cerebellum is essential for a diverse array of motor functions including coordination, learning, posture, and balance. It is therefore not surprising that damage to its circuits causes a number of motor disorders such as ataxia, dystonia, and tremor (Calderon et al., 2011; Orr, 2012; LeDoux and Lorden, 2002; Wilson and Hess, 2013; Louis et al., 2011; White et al., 2014; White et al., 2016). However, the recent intense investigation of normal and abnormal functions of the cerebellum has been directly facilitated by the wealth of knowledge about cerebellar circuitry (Ito, 2006; Glickstein et al., 2009; Sillitoe et al., 2012; Ruigrok et al., 2014; Voogd et al., 2014). With specific regards to WGA-Alexa, we used the anterograde and retrograde properties of this tracer to uncover the topographic patterning of cerebellar afferent projections in normal and mutant mice (Reeber et al., 2011a; Reeber et al., 2011b; Reeber and Sillitoe, 2011; Gebre et al., 2012; Sakai et al., 2012; Reeber et al., 2013; White et al., 2014; White et al., 2016; Sillitoe, 2016). The major benefits of the WGA-Alexa 488 (green), 555 (red), and 350 (blue) tracers for these studies were their rapid transport *in vivo*, intense brightness that facilitated whole mount imaging of the traced tissue, flexibility to be paired

with each other (multi-color tracing) or with histology and immunohistochemistry, ability to reveal long-range projections with remarkable clarity, efficiency of labeling neuronal projections and somata in developing and adult mouse brains, and limited fibers of passage problems.

Based on our previous work, here we outline the methods, steps, and reagents that we find are necessary for successful labeling of axonal projections with WGA-Alexa tracers. However, we also expand upon the technique by providing additional details for how to use the WGA-Alexa tracers in combination with: 1) a Nanoject II injector for delivering nanoliter volumes of tracer into the cerebellar system and 2) pulled glass electrodes for brightly marking localized regions of tissue after performing single-unit extracellular recordings of cerebellar neurons *in vivo*.

BASIC PROTOCOL 1

Tracing short-range topographic circuits within the cerebellum

The procedures described below use C57BL6/J inbred and Swiss Webster outbred mice purchased from The Jackson Laboratory or Taconic Biosciences, which were maintained in our animal colony. We bred the mice using timed pregnancies, and we designated noon on the day a vaginal plug was detected as embryonic day (E) 0.5. Mice of both sexes were studied at postnatal day (P) 30 or beyond. All animal studies were carried out under an approved IACUC animal protocol according to the institutional guidelines at Baylor College of Medicine.

The cerebellum is organized into a striking array of stripes called zones (White and Sillitoe, 2013). This compartmental architecture may be critical for wiring the cerebellum into specific circuits, determining neuronal functional diversity, and controlling behavior (Cerminara et al., 2015). Therefore, mapping the circuit connectivity of specific cellular populations is especially important in the cerebellum. But while the anatomy of the highly folded cerebellum is well characterized, there is much to be learned about how its functions are packaged into its precise zonal compartments. For example, subsets of lobules are patterned based on neuronal and glial populations that share specific gene expression signatures. Immunostaining with zebrinII (=aldolaseC; Ahn et al., 1994), a marker of Purkinje cell zones (Brochu et al., 1990; Sillitoe and Hawkes, 2002), reveals a pattern of zebra-like stripes in specific lobules (Apps and Hawkes, 2009; Figure 1). And although all cerebellar cell types respect this Purkinje cell gene expression organization (Consalez and Hawkes, 2013), it is unclear whether all internal projections within the cerebellum also respect the map. For instance, do clusters of granule cells project parallel fibers that respect zones of Purkinje cell dendrites in the molecular layer? This is an interesting problem to consider because anatomically parallel fibers can extend for millimeters within the molecular layer (Brand et al., 1976; Mugnaini, 1983) and therefore they would be expected to cross multiple zonal boundaries along their trajectories. It is therefore not clear where within the zonal map their distal terminals eventually come to reside. One approach to address this problem is to inject a very small amount of tracer into the cerebellar cortex to mark and map the granule cell parallel fiber axons and their terminals. Then, compare the topography of the labeled axons and terminals to the pattern of zebrinII expression in the

Purkinje cells. Here, we describe a method to mark a subset of granule cell axons *in vivo* with WGA-Alexa tracers.

General materials—Mice (We use inbred and outbred mice of both sexes that were purchased them from Jackson Laboratories (Jackson Laboratory Neurobiology, RRID:SCR_005570; Bar Harbor, MA) and Taconic Biosciences (Albany, NY) under an approved IACUC animal protocol according to the institutional guidelines at Baylor College of Medicine.)

70% ethanol (v/v)

1 mL syringe, 27 gauge needle (#301629, BD PrecisionGlide Needle, BD, Franklin Lakes NJ)

Analgesic (0.6 mg/kg buprenorphine, Buprenex Injection, Reckitt Benckiser Pharmaceuticals, NDC 12496-0757-5). We provide pre-operative and post-operative buprenorphine.

Isoflurane (delivered at 1-3%)

Isoflurane Vaporizer (Cat. # Matrx VIP 3000, Rodent Anesthesia Machine, Midmark, Versailles OH)

Anesthesia chamber (Midmark, 1.5 liter)

Surgical microscope (Zeiss Stemi 2000 with Schott Ace I light source)

DC current rechargeable heating pad (#DCT-15, Kent Scientific, Torrington, CT). *Using a DC current pad is important when combining the tracing with electrophysiological recordings, which are sensitive to electrical noise (see Basic Protocol 3).*

Eye Ointment (Celluvisc, NDC 0023-4554-30)

Povidone-iodine (BETADINE Solution Swab Aids, Purdue Pharma, Stamford, CT, USA; #67618-152-01)

Alcohol wipes (Covidien, Mansfield MA)

Hair removal cream (Nair, purchased from Walgreens)

Tools and reagents—Scalpel with disposable blades (handle no. 3, Cat. # PY2 52-3514, blades no. 10, Cat. # PY2 72-6145, purchased from Harvard Apparatus, Cambridge MA)

Small scissors (Fine Science Tools (FST), Foster City, CA, USA; FST#14082-09)

#55 forceps (FST #11255-20)

Dumont AA forceps (FST #11210-10)

Bone Drill (Ideal Micro-Drill Surgical Drills #726065)

Drill bits (Ideal Micro-Drill accessories # 726066)

Bulldog clamps (No. 18039-45, FST, Foster City, CA)

The Mouse Brain in Stereotaxic Coordinates atlas (Paxinos and Franklin, 2001 Second Edition). *For targeting specific brain regions with standard coordinates.*

David Kopf Instruments Stereotactic Rodent Frame (Tujunga CA) with non-rupture mouse ear bars (Kopf 922)

Nanoject II (Cat. No. 3-000-204, Drummond Scientific Company, Broomall PA) with Drummond capillary tubes (7” #3-000-203-G/XL) (Figure 2)

Other glass capillaries (we use Borosilicate Standard Wall without Filament, 1.5 mm OD, 0.86 mm ID, 75 mm length (# 30-00056) for spinocerebellar and other pathways when using a mechanical injection system (Reeber et al., 2011a; Reeber et al., 2011b), and we use 100 mm length, inner diameter 0.86 mm, outer diameter 1.5 mm (# 30-0060) for marking after recording (see Basic Protocol 3), both from Harvard Apparatus, Cambridge MA)

Micropipette puller (we use a Narishige PC-10 (Narishige International Inc., East Meadow NY) and a Sutter Instruments Model P-1000 Flaming/Brown micropipette puller (Sutter Instrument Co., Novato, CA))

Mineral oil (Light white, Cat. # 194836, MP Biomedicals LLC, Solon OH)

Parafilm (PM-996, Bemis, Neenah WI)

WGA-Alexa 488 and WGA-Alexa 555 (Cat. # W11261 & W32464, Thermo Fisher Scientific, Waltham MA). *We typically dilute the tracers to 2% in PBS and then store 10 µl aliquots at -20C.*

Reflex 7 stainless steel wound clips (7 mm, FST, No. 12032-07)

3M Vetbond (Purchased from Fisher Scientific #NC0304169)

Recovery chamber with heating surface (Peco Services Ltd, purchased from Harvard Apparatus, Cambridge MA)

Heat lamp (if the recovery chamber is not heated)

Avertin 1.25% solution injected at 0.025 ml/gram body weight (Cat. # 75-80-9, 2, 2, 2-Tribromoethanol, Sigma, St. Louis MO)

4% Paraformaldehyde (PFA, 441244, Sigma Aldrich, St. Louis MO). The PFA was made and stored at 20% at -20 degrees Celsius, and then diluted to 4% with PBS (see below) for use.

Sucrose (S5-3, Fisher Scientific, used at 15% and 30%)

Cryostat (Microm HM 550)

Sharpened soft lead pencil (for marking the skull)

Timer (Fisher Scientific)

KimWipes (KimTech Science, Roswell GA)

Tissue/brain molds (Cat. # 18646A, 22 × 22 × 20 mm, Polysciences Inc., Warrington PA)

Optimal Cutting Temperature (OCT) tissue embedding media (Cat. # 25608-930, Tissue-Tek, Sakura Finetek, purchased from VWR)

Phosphate buffered saline (PBS, pH 7.4). Made from PBS tablets diluted in double distilled water (P4417, Sigma, St. Louis MO)

Fisherbrand Colorfrost Plus microscope slides (Cat. # 12-550-16A, Fisher Scientific)

Vectashield mounting medium with DAPI (Vectashield H-1200, VectorLabs, Burlingame CA; Vector Laboratories Cat# H-1200 Lot# RRID:AB_2336790)

NOTE: Personal protective equipment should be used for this protocol. And since this is a sterile surgery, we carry out the tracing using sterile technique, which involves using autoclaved tools and wearing sterile personal protective equipment including a gown, gloves, and mask.

Preparation

1 Prepare glass micropipettes on puller, with parameters optimized for your target region. Extra micropipettes can be stored in a petri dish with sticky base. Never reuse a micropipette.

Our parameters for injections are as follows: heat level set at 60 on the Step 1 setting of the Narishige PC-10 Puller. The Narishige PC-10 is a downward drop puller and therefore the taper and sharpness of the electrode tip is determined by the heat that is supplied and the weight that is applied during the “drop”. Short tips for cerebellar cortex injections were pulled with 2 heavy weights and 1 light weight, while long tips for cerebellar nuclei injections were pulled with 1 heavy and 2 light weights (although we typically use the Sutter puller for finer cerebellar nuclei injections). Prior to use, the micropipette tips were clipped using forceps to ensure dispensability of neural tracer (however, this may not always be necessary).

2 Prepare surgical area. Spray down with 70% ethanol. Turn on heating pad to 37 C. Verify that the surgical microscope is positioned to focus properly without interfering with the stereotaxic frame and turn on the light source. If required, turn on heating lamp over the recovery cage to begin heating up the recovery cage. Lay out the surgical tools (but keep them within their sterile autoclaved packs within the sterile field).

3 Verify that there is sufficient isoflurane in the vaporizer and sufficient oxygen in the oxygen tank. *Note that the isoflurane machine must be regularly calibrated for optimal performance and professionally checked for leaks in the system, and changing oxygen tanks should be performed with extreme care. The scavenging system must also be regularly maintained and usage logged.*

4 Anesthetize the first mouse (if multiple mice will be worked on). Place it in the anesthesia chamber with 1-3%% isoflurane with oxygen and wait until the mouse is anesthetized.

5 Verify that the mouse is at a plane of anesthesia that is appropriate for surgery by checking for the lack of a response to a toe pinch.

6 Place the mouse on the bite bar with the nose in the nose cone connected to the isoflurane vaporizer of the stereotaxic frame. Add a small drop of eye ointment to each eye, and verify that the heating pad is warm. *Hypothermia is a major source of problems during survival surgery because the mice easily lose heat and they often fail to recover.*

7 Place ear bars carefully into the ear holes. Avoid puncturing the eardrums. Verify that each ear bar is placed an equal distance into the ear using the ruler measurement. Secure placement can be checked by lightly pressing on the skull. There should be no movement of the skull laterally or vertically – the head should only pivot forward and backward with a clean roll.

8 Remove hair from the head using Nair. Do not leave hair removal cream on skin for more than one minute to avoid “burning” the skin. Apply using a cotton tip and continuously remove cream and hair mixture in a single motion going with the grain of the hair. Remove any extra Nair after the desired patch of hair is removed. Alternatively, hair can be removed using standard electric hair clippers or a beard trimmer.

9 Sterilize the scalp by scrubbing with alcohol/Betadine. We use 70% ethanol pads to disinfect the site in preparation for incision then apply povidone-iodine (BETADINE Solution Swab Aids) to clean the skin, followed by two more rounds of ethanol/Betadine cleaning.

10 Use a scalpel to make a single, clean incision from just caudal to the eyes to the start of the musculature on the back of the neck.

11 For injecting cerebellar lobules that are deeper from the surface (for example, lobule X) or injections for tracing cerebellar nuclei projections, use fine scissors to detach and reflect apart the musculature at the base of the skull. Use clamps to hold the muscle and skin to the sides and out of the way, which also leaves the skull exposed for access (see Figure 2B, C).

Making a craniotomy

12 Secure the Nanoject II in the stereotaxic frame and use the electrode tip to find Bregma. Bregma is located at the intersection of the skull’s anatomical midline and the coronal sutures. While there is variation in Bregma across animals, it is very important to be consistent in defining Bregma. Using the x, y, and z knobs, bring the Nanoject II to the surface of the skull at Bregma. Define the zero location with the anterior/posterior and medial/lateral coordinates. Use the manipulator arm on the stereotaxic frame to move the Nanoject to the desired coordinates. Here we were targeting a region of lobule VIII in the cerebellum (Figure 3), which has coordinates of -8.7 mm, 1.1 mm, 0.5 mm.

13 Use a sharpened soft lead pencil to mark the coordinate site on the skull.

14 Remove the Nanoject II from frame. Carefully drill a craniotomy ~2mm in diameter. Remember to drill slowly through the skull. Use cotton tips to quell bleeding or if necessary use a blood vessel cauterizer if the bleeding is occurring in the soft tissues. Move very slowly when drilling through the final layer of the skull, being very careful not to excessively rip the dura mater. It is very important not to cause massive leakage of CSF.

Loading the micropipette and injecting—It is highly advised that you perform the follow steps as quickly as possible because WGA-Alexa (and other tracers) can become sticky and dry at room temperature. This makes it very challenging to eject the tracer out of the pipette, which results in little to no tracing.

15 Fill the micropipette with mineral oil, according to the Nanoject II instructions. *It is very important to avoid bubbles to ensure accurate injection volumes*. Load micropipette into the Nanoject II system, by placing the micropipette on the wire guider, which should fit snugly into the stopper. Extend the wire stopper to push out any bubbles. Verify that the secured micropipette has no bubbles. Secure the Nanoject II with the micropipette into the manipulator of the stereotaxic unit.

16 Place a square of parafilm underneath the micropipette-Nanoject II system. Pipette ~4-5 μl of tracer (in this study, we use WGA-Alexa 488 and WGA-Alexa 555 diluted to 2% in PBS) onto the square of parafilm. Set the Nanoject II speed settings and injection volume. We use the fastest speed. Using the microscope, rotate the x, y, and z knobs to lower the micropipette tip into the neural tracer bubble. Withdraw sufficient neural tracer to fill the micropipette. For example, in our test regimes when we wanted to make 150nl injections, we would withdraw ~1 μl of neural tracer. *Again, at all steps of tracer loading it is very important to prevent bubbles.*

17 Raise the micropipette tip out of the neural tracer bubble, using the z knob. Perform one short test injection to verify that the tracer can be ejected through the micropipette tip. Remove parafilm.

18 If an angled point of entry is desired, angle the micropipette here. For deep cerebellar nucleus injections, we angle the micropipette to 40 ° (see Figure 2). Using the loaded micropipette, re-zero A/P, and M/L coordinates at Bregma, without directly touching the skull. Move the micropipette to the injection coordinates. Carefully bring the tip of the micropipette to the surface of the brain, without penetrating the tissue. Zero the D/V coordinate.

19 Slowly lower the Nanoject II to the desired D/V coordinate. To optimize complete neural tracer delivery, overshoot the D/V coordinate by 0.01 mm, then return to the exact coordinate. This creates a pocket with negative pressure that helps the neural tracer to enter the tissue.

20 Minimal diffusion is achieved by injecting 10 nl injections, spaced out with 15 seconds intervals. For large WGA-Alexa injections, we typically inject up to a

total volume of 150 nl, and small injections between 20-50 nl. Set the timer to count up, to ensure evenly spaced injections.

21 When the injection is completed, move the Nanoject II in and out quickly within +/− .01 mm, to clear any potential clogging (although for small targets be careful not to damage the site). Use the timer to leave the Nanoject II in the tissue for >2 minutes following the injection to allow all neural tracer to enter the tissue.

Closing up and recovery

22 Use 4-5 wound clip staples to close the incision. Sparingly apply Vetbond to help seal the skin. Keep in mind that Vetbond dries quickly yet initially it is very fluid. Be careful to avoid Vetbond reaching the eyes of the animal. *And of course, the experimenter must also be careful to not get Vetbond onto their skin or into their eyes.*

23 Turn off isoflurane and place the mouse in the heated recovery cage. Allow the mouse to fully wake up and begin exploring the cage before returning it to the home cage. *Post-operative care is essential for the mouse to recover properly and a critical part of every survival surgery experiment.*

24 Clean up the surgical station, throw all biohazardous tissue in appropriate waste and clean area with 70% ethanol. Tools can be sterilized using a glass bead sterilizer between mice during the same surgery session or cleaned and autoclaved for another day.

Perfusion and tissue processing

25 Schedule a perfusion according to the neural tracer selected and the amount of tracing desired. Minimal incubation time for WGA-Alexa is in the range of hours. However, the intensity of labeling within a given period of time depends on the length of the tract.

26 Anesthetize the mouse with Avertin or your approved method. Wait until the toe pinch reflex is completely abolished before beginning the perfusion procedure.

27 Flush the blood out of the mouse by driving it with the transcardiac method using PBS pH 7.4 (or saline) and then perfuse the tissue using 4% PFA.

28 Dissect the brain and then post-fix it overnight in 4% PFA. The following day, put the brain into a 15% sucrose solution diluted in PBS until the brain sinks to the bottom of the container. Next, move the brain into a 30% sucrose solution diluted in PBS, again until the brain sinks. It is now cryoprotected and ready for freezing.

29 Dry the brain gently on a KimWipe, then mount the brain in OCT and immediately freeze at -80°C for >1.5 hours prior to sectioning.

30 Cut 40 μm sections on a cryostat at −20°C.

31 For free-floating immunohistochemistry, collect tissue sections in a 24 well plate filled with PBS. Here, zebrinII was used at 1:250 (kind gift from Dr. Richard

Hawkes; R. Hawkes, University of Calgary; Alberta; Canada Cat# ZebrinII Lot# RRID:AB_2315622; Figure 4). Please see our previous publications for additional details on our specific procedures for immunohistochemistry (Sillitoe and Hawkes, 2002; Sillitoe et al., 2010; White et al., 2014; White et al., 2016a; White et al., 2016b).

32 For mounting, add a few drops of Vectashield to preserve the fluorescent signal, and then gently lay a glass coverslip over the slide.

33 WGA-traced samples can be immediately mounted onto a glass slide and imaged. WGA-Alexa signal declines quickly and by 3 days after sectioning minimal signal is left for imaging.

34 Image the tissue on any epifluorescent or confocal microscope. We capture our photomicrographs of tissue sections using Zeiss AxioCam MRm (fluorescence) and AxioCam MRc5 (brightfield) cameras mounted on a Zeiss Axio Imager.M2 microscope, which is equipped with Zeiss CY3 (model #41007a), FITC (model #41001), and DAPI/Hoechst/AMCA (model #31000v2) filters. Images of tissue sections were acquired and analyzed with Zeiss AxioVision software (release 4.8) or Zeiss ZEN software (2012 edition; ZEN Digital Imaging for Light Microscopy, RRID:SCR_013672). The raw data were imported into Adobe Photoshop CS5 and corrected for brightness and contrast levels.

BASIC PROTOCOL 2

Tracing long-range topographic projections from the spinal cord to the cerebellum

The spinocerebellar tract is one of the longest tracts in the mammalian nervous system. It carries proprioceptive and fine touch signals from all levels of the spinal cord directly to the cerebellum (Bosco and Poppele, 2001). Within the cerebellum, the tract terminates bilaterally with an ipsilateral predominance. Interestingly, the terminal field organization of mossy fibers in the cerebellum respects the pattern of Purkinje cell zones. Spinocerebellar afferents terminate into parasagittal zones in the granule cell layer of lobules I-V and lobules VIII-IX (Voogd et al., 1969; Gravel and Hawkes, 1990; Grishkat and Eisenman, 1995; Vogel and Prittie, 1994; Vig et al., 2005; Sillitoe et al., 2010; Reeber et al., 2011a). We used the Nanoject II delivery approach to examine the termination pattern of the spinocerebellar projections after delivering a controlled volume of WGA-Alexa 555 into the spinal cord of adult mice (Figure 5). WGA-Alexa tracers are also ideal for examining the topography of different pathways. To demonstrate this, we injected WGA-Alexa 488 into the lower thoracic-upper lumbar spinal cord and WGA-Alexa 555 into the external cuneate nucleus (see Gebre et al., 2012). The resulting anterograde tracing revealed the complementary topographic targeting of cuneocerebellar (forelimb sensory information) and spinocerebellar (hindlimb sensory information) mossy fiber pathways into a series of adjacent terminal field domains in the granule cell layer (anterior cerebellum shown in Figure 6).

Note however that similar to WGA and its conjugates, WGA-Alexa 555 also travels in the retrograde direction (Reeber et al., 2011b; Sakai et al., 2012). Here, when we performed injections into the lower thoracic-upper lumbar region of the spinal cord we could

retrogradely label inferior olive neurons in the ventral brainstem (Figure 5C). At the cellular level, upon retrograde transport into olivary neurons, the tracer travels into the somata where the WGA-Alexa 555 molecule tends to accumulate in small punctate deposits (Figure 5D). The retrogradely traced cell bodies are therefore easy to identify.

Materials—Please refer to the Materials and general Steps for surgery that were described for Basic Protocol 1. However, instead of a craniotomy, to access the spinal cord we performed a dorsal laminectomy (Reeber et al., 2011a; Reeber et al., 2011b). We then injected 20nl of WGA-Alexa 555 using the Nanoject II onto each side of the the lower thoracic-upper lumbar region of the spinal cord over a 5 min period. The mice were perfused 24 hours later, 40 μm tissue sections cut on a cryostat, and the tracing visualized by directly imaging the spinocerebellar fibers and terminals within the cerebellum or the somata in the inferior olive. For further details of spinocerebellar tracing in development, adult, and studies of mutant mice please refer to our previous work (Reeber et al., 2011a; Reeber et al., 2011b; Gebre et al., 2012; Sakai et al., 2012; White et al., 2014; White et al., 2016a; Sillitoe, 2016).

BASIC PROTOCOL 3

Local and rapid marking of neural tissue after *in vivo* extracellular single-unit recordings

Studies that pair structure and function analyses are incredibly informative for understanding how neural circuits control behavior. One method to achieve this is to examine neural function with a clear and precise idea of the anatomical structure being studied. We used the cerebellar nuclei to demonstrate the power of marking specific regions after recordings were performed *in vivo*. The cerebellum contains more than half the number of neurons in the entire brain and therefore with so many neurons and with such diverse electrophysiological properties recording “blindly” can often make data interpretation challenging. To overcome this challenge, we demonstrate how to locally mark neurons with WGA-Alexa immediately after recording. We use the cerebellar nuclei because they are nestled amongst numerous white matter tracts within the core of the cerebellum (Sillitoe et al., 2012). There are three pairs of cerebellar nuclei, the fastigial (medial), interposed (middle), and dentate (lateral). Together, the three divisions of the cerebellar nuclei constitute the primary output of the cerebellum. The individual nuclei are often difficult to target and confirm during a recording, especially when the cells have been genetically manipulated and take on unexpected firing phenotypes (White et al., 2014). Clearly marking the recording site eliminates some of these ambiguities.

Materials (electrophysiology)—Single-unit recordings are attained with 1-3 MΩ glass electrodes (please see below) controlled by a motorized micromanipulator (MP-225; Sutter Instrument Co., Novato, CA). Signals are band-pass filtered at 0.3-13 kHz, amplified with an ELC-03XS amplifier (NPI Electronic Instruments, Tamm, Germany), and then digitized (CED Power1401) and recorded using Spike2 software (CED, Cambridge, UK). For quantitative analysis we collect continuous traces of >300 seconds and examine spikes with Spike2 (Spike2 Software, RRID:SCR_000903), MS Excel, and MATLAB (Mathworks, Natick, MA). Please refer to our recent work for additional details on electrophysiology and

the methods for analysis of spike properties (Arancillo et al., 2015; White et al., 2014; White et al., 2016b).

1. WGA-Alexa 488 (or WGA-Alexa 555) is diluted to 1% in a 100 ul 0.9% saline solution.
2. We fill low-impedance (1-3 MΩ), pulled borosilicate glass electrodes (GC150F-10, 1.5 OD X 0.86 ID X 100 L mm, Harvard Apparatus, Cambridge MA) with the WGA-Alexa solution. For these electrodes in this application we set our Sutter Instruments Micropipette Puller to a ramp of 500.
3. A craniotomy is opened over the cerebellum (as described above), and the electrode is inserted into the cerebellar nuclei based on stereotaxic coordinates. For this experiment, we used 6.075 mm posterior, 1.911 mm lateral, and 2 mm from surface of the brain, which targeted the interposed cerebellar nuclei (Figure 7).
4. Single neurons were isolated based on their expected firing rate (White et al., 2014), and then recorded for at least 300 seconds (Figure 7C). The quality of the single-unit recordings was examined post-hoc using principle components analysis.
5. After recording, we begin pulsing a 500 ms (square pulse) positive 25 nA current, then 500 ms of no stimulation. This sequence is repeated for ~ 1 hour. Throughout this procedure we check and ensure that the isolated cell continues firing throughout stimulation; healthy neurons are more likely to take up tracer when it is delivered using a current. We then stop the stimulation and let the brain sit without manipulation for ~ 90 minutes to allow the marked tissue with the traced cells to equilibrate before sacrificing the animal.
6. As described above, while the mouse is still under full anesthesia (although in this case after recording neurons) we first flush the blood with PBS and then perfuse with 4% PFA. We then allow the brain to post-fix overnight in 4% PFA before beginning a two day cryoprotection protocol of 15% sucrose the first day, and then 30% the second. Then brain is then sectioned coronally, and then mounted using Vectashield or FluoroGel. The mounting medium is given ~30 minutes to dry in the dark at 4 degrees Celsius. The sections are then imaged immediately since the brightness of the traced cells declines rapidly on sections (Reeber et al., 2011a). *Thus, the best way to store the tissue is to leave the brain in 4% PFA. Only when images can be immediately captured should the experimenter cryoprotect and cut the brain.*

COMMENTARY

Neural tracing is a valuable tool for elucidating synaptic connectivity and circuitry throughout the central nervous system. Lectin-based tracers have become a staple neuroanatomical tool (Mesulam, 1982). WGA tracing of populations of cells has been achieved using neural tracers across distances as long as a mouse spinal cord (Reeber et al., 2011a; Reeber et al., 2011b). However, the resolution of tract tracing is limited by the

delivery volume and precision of injection. Moreover, it is difficult to gather functional information of traced neurons. Here, we describe a technique for tracing local groups of targeted neurons by injecting nanoliter volumes of WGA-Alexa to precise regions using the Nanoject II pressure-injection system with a stereotaxic frame for accurate and precise delivery. We discuss how stereotaxic guided neural tracing can be used to study cerebellar circuitry, although this versatile tool can be applied to answer questions in other neural systems.

Background Information

WGA enters neurons by diffusion near the injection site, although it also enters the surrounding cells by endocytosis. WGA is incorporated into these cells via adsorptive-mediated endocytosis upon binding to the surface receptors (Dumas et al., 1979b; Mesulam, 1982). Once it enters, the WGA is actively transported in vesicles, which allows it to distribute to all regions of a cell, and in neurons this includes the axons and dendrites. Because of this generalized and global method of transport, within the cell it can travel in both the anterograde and retrograde directions. But, it also can cross the cell's synaptic compartments and eventually enter into connected cells from either end of the neuron (terminals on axons or synapses on dendrites) (Mesulam, 1982). In neurons, this mode of cell-to-cell transfer is referred to as transynaptic. WGA conjugate tracers have been demonstrated to travel transneuronally in the nervous system of different species including mouse (Sillitoe, 2016) and chicken (Gerfen et al., 1982).

Although WGA revolutionized brain circuit analysis, it has not come without its challenges. It can be difficult to attain reliable staining with WGA, and one major reason for this is that by itself, its sensitivity is in fact relatively low. To overcome this problem, WGA was conjugated to HRP (horseradish peroxidase) (Gonatas et al., 1979; Mesulam, 1982; Staines et al., 1980). HRP itself is an easy to use and effective tracer (Mason and Gregory, 1984), but its conjugation to form WGA-HRP produced cleaner tracing results, and therefore the pairing of the two tracers plus improved methods of detecting the signal generated a more reliable tool (Mesulam, 1982). In the decades to follow, many studies used WGA-HRP, with many of those studies conducted in the cerebellum (Vogel and Prittie, 1994; Sillitoe et al., 2010). WGA-HRP has been successfully used to trace projections in different brain systems in a long list of model organisms including rodents, cats, and monkeys (Peschanski and Ralston, 1985; Itaya et al., 1986; Quigg et al., 1990; Herzog and Kummel, 2000; Erichsen and May, 2002).

Despite the incredible advances in the last two decades that have catapulted our understanding of brain structure and function (viral tracing, optogenetics, conditional genetics, imaging, *in vivo* electrophysiology), still, there is a pressing need to resolve the fundamental wiring diagram of the brain. The many "BRAIN" initiatives that have started all over the world underscore this idea. To address the anatomical basis of the brain from a systems level, one method would be to simultaneously label multiple pathways in the same animal, and then view the precise trajectories and connectivities of the different pathways at high resolution, in 3-dimensions. To start to address this problem, we developed a WGA based approach to track and map the highly patterned circuit connectivity in the mouse

cerebellum (Reeber et al., 2011a, Reeber et al., 2011b). When we initiated these studies, we thought that for our approach to be beneficial for studying complex circuit diagrams, we might need to fulfill three major criteria: 1) rapid labeling of short- (within the cerebellum) and long- (afferents and efferents of the cerebellum) range pathways, 2) clear and full visibility of individual axon trajectories and their terminals (for example, the “rosette” in the mossy fiber terminals), and 3) bright fluorescent tag for visualizing multiple fiber types even at lower magnification, for simultaneous analysis of multiple tracts in the same animal, and for combinatorial use with other marker tools such as antibodies. Using the spinocerebellar tract as a model we identified a line of WGA conjugated Alexa fluorophore tracers (WGA-Alexa 555 *red*, WGA-Alexa 488 *green*, and WGA-Alexa 350 *blue*; Invitrogen/Life Technologies, NY) for labeling brain circuits (Reeber et al., 2011b). We reported that in adult mice, the long lumbar spinocerebellar axons and their associated terminals within the cerebellum could be traced in their entirety in less than six hours from the time of injection. In addition, individual axons were visible along the trajectory in the white matter and the glomerular structure of rosettes was easily identifiable within the gray matter of the cerebellum (Reeber and Sillitoe, 2011). We could label multiple pathways in the same animal (Reeber et al., 2011b; Figure 6), and remarkably we could image adult spinocerebellar terminals more than 150 μm below the pial surface from the surface of the cerebellum, in intact fixed cerebella (Reeber et al., 2011b). Importantly, the “fibers of passage” problem (Mesulam, 1982), which is a major problem for many tracers, is not an issue with WGA-Alexa. For example, within the cerebellar peduncles, axons labeled with red, green, and blue WGA-Alexa were found to travel close to one another, without any indication of inappropriate transfer of tracer between axons (Reeber et al., 2011b). Importantly, WGA-Alexa can travel transynaptically and it brightly labels the neurons that are connected to the traced axons (Goshgarian and Buttry, 2014; Sillitoe, 2016). In addition to its anterograde tracing properties, we have shown that WGA-Alexa 555, much like the other WGA conjugates, can travel retrogradely (Reeber et al., 2011b; Sakai et al., 2012; Figure 5). This can introduce several considerations (please see **Other limitations** below), although there are clear advantages to having a dual tracer. If the circuitry of a specific region is completely unknown, then as a starting point the ability to trace in both directions can reveal a massive amount of information about what is coming in and what is going out of that particular location. The anterogradely traced fibers are easy to identify because the tracer fills the axons and it tends to travel into the terminals where it can fill large terminals with clarity. The anterogradely traced profiles can be distinguished from the retrogradely traced somata because the WGA accumulates into punctate deposits that are scattered throughout the somata. This feature of the tracing can be easily appreciated in medium to large sized neurons in the inferior olive (Figure 5). Clearly though, you lose the resolution of tracing distinct pathways because when viewed from the perspective of the injection locus, its afferent (retrograde) and efferent (anterograde) axons will be labeled. In this scenario, distinguishing the two projection types is challenging, and in many cases impossible, especially proximal to the injection.

Critical Parameters and Troubleshooting

Neural tracer delivery parameters can be adjusted to further control the degree of diffusion at the delivery site, the extent of neural tracing and the size of the region targeted. The volume

delivered will directly affect the amount of spreading and diffusion at the injury site. In this protocol, we use the Nanoject II system, originally designed for oocyte injections. However, this system can be adapted to a stereotaxic frame to provide accurate targeting combined with the benefit of nanoliter volume control. WGA typically displays more diffusion compared to other tracers such as BDA. Therefore, adjusting incubation times controls the degree of circuit tracing. We generally suggest injecting smaller volumes for a longer period of time to improve the extent of neural tracing. It is also important to consider the size of the region of interest when preparing the glass micropipette tips that conform to the Nanoject II system. A variety of micropipette puller systems can reproducibly control the diameter, length, and taper of the micropipette tip (Narishige Puller System, Sutter Instruments Micropipette Puller, see Sutter Instrument Puller Cookbook). Adjusting these parameters can enable control of the stability of the tip, which in turn affects the degree of tissue damage. This is important to consider when using WGA since some tissue damage is actually helpful in getting the tracer into cells – although too much damage will destroy the neurons which negatively impacts tracer uptake, and if it does get taken up the cells could still die due to excessive damage. Additionally, micropipettes can be designed with longer and finer tips, which are ideal for penetrating deeper tissues. While long, thin micropipette tips will minimize tissue damage along the entry tract, more pressure and speed will be necessary to deliver the tracer along the narrow tip to the tissue. One should also consider micropipette diameter when designing the experiment. Larger diameters facilitate increased diffusion and targeting of broader regions. Smaller diameters can target regions as local as a single layer in the cerebellar cortex (Figure 3).

In addition to labeling tracts, thin diameter (sharp) electrodes are used for isolating single neurons for electrophysiological analysis. However, because the studies we described here are conducted *in vivo*, thin glass electrodes tend to break both during the Nanoject II injections and the recording experiments. To overcome this problem, it is advised that better stability of the mouse, particularly the head, should be achieved (White et al., 2016b). This will reduce small sudden movements that often crack or break the glass electrode tips. Also, it is important to empirically determine the sufficient sharpness and length of the electrode required. If the electrodes continue to break even with excellent stability, then a slightly thicker or less tapered electrode might be better, or perhaps choose a glass capillary with a slightly thicker wall diameter (you can keep the total diameter the same if the targeted area is very small).

Unfortunately, sometimes the results of the tracing may be inadequate, even if the glass electrodes were designed correctly and performed effectively during the procedure. One might observe too few marked axons, or no labeling at all, there may be a very large injection site with local staining of tracer but no actual tracing of axons, or there may be no indication of tracing at all. It is possible that the tracer simply did not leave the pipette, or too little was ejected. Using larger bore capillaries could address these problems, as described above. Or, in many cases these problems can be solved by working a little faster once you get to the pipette filling stage. WGA and its conjugates are “sticky” and often they adhere to the glass as they dry. However, if only a few axons are labeled, then injecting more WGA-Alexa could be helpful. But, leaving the electrode in the tissue after ejecting the tracer for an extended period of time could be helpful since this gives the tissue a longer time to

equilibrate and also provides the tracer with a period when it can enter the cells without tissue movements – the tissue moves once the glass electrode is withdrawn, which can displace tracer. Also, it can be very helpful during injection to advance the tip a little farther than you need (by a matter of microns) and then reverse before injecting. This creates a reservoir that can help hold your tracer within a restricted area of tissue, which allows it to remain at the desired site with minimal disturbance.

Statistical Analyses

Here we presented the raw spike data as a way of qualitatively demonstrating the isolation of a cerebellar nuclear neuron and then marking the site with WGA-Alexa 488 (Figure 7). However, the spikes can be analyzed for a number of different measures including frequency (Hz = spikes/s), interspike intervals' (ISI) coefficient of variance (CV = (standard deviation of ISIs)/(mean of ISIs)), and CV2, (CV2 = 2|ISIn+1–ISIn|/(ISIn+1+ISIn)) (Holt et al., 1996). Calculations are typically reported as mean ± standard error of the mean (SEM). Routine spike analyses make use of unpaired, two-tailed Student's t-tests or ANOVA, although many tests can be done depending on the experiments that are performed. For several examples of spike analysis please refer to our previous work (Arancillo et al., 2015; White et al., 2014; White et al., 2016a; White et al., 2016b). WGA-Alexa is valuable for tracking projections and examining the patterns of terminal distribution, although quantitative puncta analysis could be performed, as typically done for immunohistochemical staining of synaptic terminals (White et al., 2014).

Understanding Results

Stereotaxic coordinates accurately direct injections to targeted locations—We confirmed consistent targeting of WGA-Alexa at two fundamental points in the cerebellar circuit: the granule cell layer (mossy fiber terminals and granule cell axons) and the cerebellar nuclei. We targeted lobules VIII and IX in order to begin exploring how the internal circuitry of the cerebellum is parcellated. The Nanoject technique offers the opportunity to inject a neural tracer into a single cerebellar layer, which could provide insight into zonal connectivity with cluster-specific resolution. The well-characterized zonal patterning marker zebrinII (Sillitoe and Hawkes, 2002) has obvious domains in lobules VIII and IX. The sharpness of zonal boundaries in this area is useful when targeting discrete circuits. Moreover, we already know that the spinocerebellar fiber tracts terminate in lobules VIII and IX (Gravel and Hawkes, 1990; Vogel and Prittie, 1994; Sillitoe et al., 2010; Reeber et al., 2011a), they respect the zebrin pattern (Gravel and Hawkes, 1990; Reeber et al., 2011b), and within this architecture exists the circuitry for controlling locomotion and proprioception (Bosco and Poppele, 2001; White et al., 2014). Thus, together with our WGA-Alexa spinocerebellar tracing (Figure 5), we expected the cluster-restricted granule cell targeting of the WGA-Alexa tracer (Figure 3, 4) to reveal new clues for how movement circuits in the posterior cerebellum are organized for function. Indeed, using an elegant combination of electrophysiology and imaging, a recent study uncovered a functional correlate for granule cell synaptic connectivity to cerebellar cortical modules (Valera et al., 2016). Interestingly, the finding that granule cell patches connect to distant modules is in accordance with our WGA-Alexa tracing data showing that labeled subsets of parallel fibers project and terminate at zebrinII zones that are located hundreds of microns away (Figure 4).

Although, it is interesting that Purkinje cells were only rarely retrogradely traced after targeting the injections into the granular layer. It could be that our injections damaged the Purkinje cell axons to a degree that passing fibers could not effectively take up the tracer.

Injections are precise and accurate, lending to flexibility in multi-injection experiments—We were successful in making the injection sites small and localized (Figure 3). Diffusion was minimized by determining the optimal volume (up to 150 nl, injected in increments of 10 nl every 15 seconds), pressure injection speed ("fast", 46 nl/sec) and micropipette tip size. Diffusion was further tested and controlled by delivering a predetermined volume of tracer over a series of smaller injections spaced temporally. We further optimized tracer delivery by creating a negative pressure pocket of air at the injection site, as described in the protocol.

The small injections of WGA-Alexa were targeted to the lateral margin of the vermis or hemisphere in the granular cell layer of lobule VIII. Precision in targeting injections enabled us to explore multi-injection experiments. Two injections made in close proximity to one another were successfully performed (Figure 3). The closely spaced injections were possible due to the small injection size and associated clean injection hole (a result of the small capillary tip and gentle injection process). Furthermore, we were able to inject tracer plus a marker to visualize different features of the circuit. WGA-Alexa 488 was injected simultaneously with fast green. The fast green can be seen at the lateral margins of lobule VIII on a wholemount (Figure 3A).

Our previous results showed strong WGA tracing at 3 days (Reeber et al., 2011a), although we successfully traced the entire spinocerebellar tract within 6 hours using WGA. Note however that Reeber and colleagues used a mechanical pressure injection system, which can lead to more tissue damage than the less forceful Nanoject II system used here, and thus likely requires more time for tracer uptake. But, the large volumes delivered by the mechanical system can be ejected and bulk loaded into the target at a rapid rate. Still, less tissue damage using the Nanoject II is an advantage that preserves the circuit anatomy close to the injection site.

Preserving circuit anatomy is particularly important for examining structure-function relationships in the brain. We tested this idea by locally labeling circuits in the cerebellar nuclei after recording the neurons *in vivo*. After marking and recording neurons with a sharp glass electrode, further detailed analysis may be performed. This includes immunohistochemistry and gene expression analysis, or perhaps even RNA sequencing at the single-cell level.

Time Considerations

Survival neurosurgeries have to be conducted with care. Accordingly, these procedures are time consuming. In general, we would assume that with a reasonable amount of practice that the Nanoject II injection surgeries should take 30-45 minutes each. Making a craniotomy for *in vivo* recordings should take 20-30 minutes. However, with practice these times can be substantially decreased. And if available, help from a colleague during the procedures can

speed up the time, which would improve the quality of the surgery and ultimately even survival rate.

It is also helpful to spend about 2-3 hours the day before the surgery preparing the surgery area, pulling glass electrodes, aliquoting WGA-Alexa, and autoclaving any necessary tools.

We previously performed a time course analysis in control mice to determine how rapidly WGA-Alexa tracers are transported in the spinocerebellar system (Reeber et al., 2011a). We did not observe any staining after 1 h of tracing, and only scattered deposits of WGA-Alexa were seen after allowing 3 h of tracing. But, allowing the tracer to travel for 6 h after injection was enough time for WGA-Alexa 555 to travel and get deposited into mossy fiber terminals. This was also sufficient time to reveal the general architecture of the spinocerebellar zonal map. By 12 h, the mossy fiber zonal map was more clearly resolved. And by 24 h, each “band” or zone in the pattern was heavily deposited with WGA-Alexa tracer and the full map was obvious. We could detect only minimal differences in the overall staining intensity within each terminal field zone after 24, 48, and 72 h of tracing. And for marking neurons after recording, 30 minutes is enough to label a small region, although a more intense and reliable spot is detected after 1 h.

Other limitations

Although WGA-Alexa tracing is an excellent technique for several reasons such as its use in experiments that require rapid anatomical tracing and it provides a bright signal that allows for multi-color tracing (Gebre et al., 2012; Reeber et al., 2011b), some limitations should be considered when designing experiments. First, the retrograde tracing properties of WGA-Alexa may complicate circuit analysis (Figure 5). Specifically, one challenge of retrograde tracers, in general, is the limited accuracy in determining which terminals, in what specific part of the injection spot (which can be large), are responsible for taking up the tracer before it is retrogradely transported. Second, the simultaneous anterograde and retrograde transport of WGA-Alexa may complicate circuit analysis for certain circuit configurations. Namely, when analyzing an anterograde pathway there is the possibility of retrogradely labeling neurons that project to that specific injection site, which in turn could have axon collaterals to a second (or perhaps to even a third) site, which would not arise from the neurons at the injection site. In this scenario it becomes very difficult to discern the connectivity and the anterograde versus retrograde direction of information flow in the labeled processes.

While WGA-Alexa tracing provides a rapid (hours to days) bi-directional labelling approach compared to viral vectors, which typically require weeks for complete expression, WGA tracing does not confer cellular specificity whereas viral vector tracing can include cell-type specific promoters to selectively target and trace cells within a circuit. However, in experimental designs that require the identification of a particular cell type, immunostaining of tissue sections can be performed to identify the neurons of interest. Co-labeling using markers plus examining the 555/488/350 fluorescent tags on the WGA-Alexa traced neurons can achieve this. Since the WGA signal densely labels the injection site, experimental questions investigating cell-type specific tracing near the injection might be better addressed using a different tracer such as BDA or by injecting smaller volumes of WGA to facilitate co-labelling studies using immunostaining.

The problem of what is going on at the injection site is not limited to the retrograde tracing properties. In our experience, WGA-Alexa is extremely valuable for examining the topography of different projections. But, when used in this manner the size of the injection spot can be large, and the precise identification of neurons that give rise to the anterogradely traced fibers is challenging. In this regard, this is a major advantage of the PHA-L technique (Gerfen and Sawchenko, 1984) or AAV-viral based tracing methods (Arenkiel, 2015). Despite the various shortcomings that each tracer might have, the identification of additional tracers is broadening the toolkit with which to study brain pathways. Therefore, before initiating an experiment, it is helpful to delineate the experimental requirements to fully address the problem and the analyses to be undertaken. Only then can the appropriate tracer (or tracers) be chosen, but still keeping in mind the background knowledge of what can be interpreted and what cannot.

Acknowledgments

This work was supported by funds from Baylor College of Medicine (BCM) and Texas Children's Hospital. R.V.S. received support from The Bachmann-Strauss Dystonia and Parkinson Foundation, Inc., The Caroline Wiess Law Fund for Research in Molecular Medicine, BCM IDDRC U54HD083092, National Center For Research Resources C06RR029965, and the National Institutes of Neurological Disorders and Stroke (NINDS) R01NS089664. J.J.W. received support from NINDS F31NS092264. The BCM IDDRC Neurovisualization Core performed a portion of the immunohistochemistry and histology experiments (supported by U54HD083092). The content is solely the responsibility of the authors and does not necessarily represent the official views of the National Center For Research Resources or the National Institutes of Health (NIH). S.L.L. and R.V.S. designed the experiments. S.L.L., J.J.W., E.P.L., and L.S. performed the experiments. S.L.L. and R.V.S. wrote the paper.

LITERATURE CITED

Ahn AH, Dziennis S, Hawkes R, Herrup K. The cloning of zebrin II reveals its identity with aldolase C. Development (Cambridge, England). 1994; 120(8):2081–90.

Apps R, Hawkes R. Cerebellar cortical organization: a one-map hypothesis. Nature Reviews Neuroscience. 2009; 10(9):670–681. [PubMed: 19693030]

Arenkiel, BR., editor. Neural Tracing Methods. Springer; 2015.

Borges LF, Sidman RL. Axonal transport of lectins in the peripheral nervous system. The Journal of Neuroscience. 1982; 2(5):647–653. [PubMed: 6176698]

Bosco G, Poppele RE. Proprioception from a spinocerebellar perspective. Physiological Reviews. 2001; 81(2):539–568. [PubMed: 11274339]

Brochu GIN, Maler L, Hawkes R. Zebrin II: A Polypeptide Antigen Expressed Selectively by Purkinje Cells Reveals Compartments in Rat and Fish Cerebellum. Journal of Comparative Neurology. 1990; 291:538–552. [PubMed: 2329190]

Brand S, Dahl AL, Mugnaini E. The length of parallel fibers in the cat cerebellar cortex. An experimental light and electron microscopic study. Experimental Brain Research. 1976; 26(1):39–58. [PubMed: 61126]

Calderon DP, Fremont R, Kraenzlin F, Khodakhah K. The neural substrates of rapid-onset Dystonia-Parkinsonism. Nature Neuroscience. 2011; 14(3):357–365. [PubMed: 21297628]

Cerminara NL, Lang EJ, Sillitoe RV, Apps R. Redefining the cerebellar cortex as an assembly of non-uniform Purkinje cell microcircuits. Nature Reviews Neuroscience. 2015; 16(2):79–93. [PubMed: 25601779]

Consalez GG, Hawkes R. The compartmental restriction of cerebellar interneurons. Frontiers in Neural Circuits. 2012 Jan.6:123. [PubMed: 23346049]

Coulter J, Sullivan M, Ruda M. Lectins as markers for studies of neuronal connectivity. Society for Neuroscience Abstract. 1980; 6:339.

Dumas M, Schwab ME, Thoenen H. Retrograde axonal transport of specific macromolecules as a tool for characterizing nerve terminal membranes. Journal of Neurobiology. 1979; 10(2):179–197. [PubMed: 512657]

Erichsen JT, May PJ. The pupillary and ciliary components of the cat Edinger-Westphal nucleus: a transsynaptic transport investigation. Visual Neuroscience. 2002; 19(1):15–29. [PubMed: 12180856]

Gebre SA, Reeber SL, Sillitoe RV. Parasagittal compartmentation of cerebellar mossy fibers as revealed by the patterned expression of vesicular glutamate transporters VGLUT1 and VGLUT2. Brain Structure & Function. 2012; 217(2):165–180. [PubMed: 21814870]

Gerfen CR, O'Leary DDM, Cowan WM. A note on the transneuronal transport of wheat germ agglutinin-conjugated horseradish peroxidase in the avian and rodent visual systems. Experimental Brain Research. 1982; 48(3):443–448. [PubMed: 6185358]

Gerfen CR, Sawchenko PE. An anterograde neuroanatomical tracing method that shows the detailed morphology of neurons, their axons and terminals: immunohistochemical localization of an axonally transported plant lectin, Phaseolus vulgaris leucoagglutinin (PHA-L). Brain Research. 1984; 290(2):219–238. [PubMed: 6198041]

Glickstein M, Strata P, Voogd J. Cerebellum: history. Neuroscience. 2009; 162(3):549–559. [PubMed: 19272426]

Goldstein I, Hayes C. The lectins: carbohydrate-binding proteins of plants and animals. Advances in Carbohydrate Chemistry and Biochemistry. 1978; 35:127–340. [PubMed: 356549]

Gonatas NK, Harper C, Mizutani T, Gonatas JO. Superior Sensitivity of Conjugates of Horseradish Peroxidase with Wheat Germ Agglutinin for Studies of Retrograde Axonal Transport. The Journal of Histochemistry and Cytochemistry. 1979; 27(3):728–734. [PubMed: 90065]

Goshgarian HG, Buttry JL. The pattern and extent of retrograde transsynaptic transport of WGA-Alexa 488 in the phrenic motor system is dependent upon the site of application. Journal of Neuroscience Methods. 2014; 222:156–164. [PubMed: 24239778]

Gravel C, Hawkes R. Parasagittal organization of the rat cerebellar cortex: Direct comparison of Purkinje cell compartments and the organization of the spinocerebellar projection. Journal of Comparative Neurology. 1990; 291(1):79–102. [PubMed: 1688891]

Grishkat HL, Eisenman LM. Development of the spinocerebellar projection in the prenatal mouse. Journal of Comparative Neurology. 1995; 363(1):93–108. [PubMed: 8682940]

Herzog J, Kümmel H. Fixation of transsynaptically transported WGA-HRP and fluorescent dyes used in combination. Journal of Neuroscience Methods. 2000; 101(2):149–156. [PubMed: 10996375]

Itaya SK, Van Hoesen GW, Barnes CL. Anterograde transsynaptic transport of WGA-HRP in the limbic system of rat and monkey. Brain Research. 1986; 398(2):397–402. [PubMed: 3801912]

Ito M. Cerebellar circuitry as a neuronal machine. Progress in Neurobiology. 2006; 78(3–5):272–303. [PubMed: 16759785]

Larsell O. The morphogenesis and adult pattern of the lobules and fissures of the cerebellum of the white rat. Journal of Comparative Neurology. 1952; 97:281–356. [PubMed: 12999992]

Ledoux MS, Lorden JF. Abnormal spontaneous and harmaline-stimulated Purkinje cell activity in the awake genetically dystonic rat. Experimental Brain Research. 2002; 145(4):457–467. [PubMed: 12172657]

LeVine D, Kaplan MJ, Greenaway PJ. The purification and characterization of wheat-germ agglutinin. The Biochemical Journal. 1972; 129(4):847–856. [PubMed: 4655820]

Louis ED, Faust PL, Vonsattel JPG. Purkinje cell loss is a characteristic of essential tremor: Towards a more mature understanding of pathogenesis. Parkinsonism and Related Disorders. 2012; 18(8): 1003–1004. [PubMed: 22795481]

Mason CA, Gregory E. Postnatal maturation of cerebellar mossy and climbing fibers: transient expression of dual features on single axons. The Journal of Neuroscience. 1984; 4(7):1715–1735. [PubMed: 6737039]

Mesulam, M. Neural Connections with Horseradish Peroxidase. Mesulam, M., editor. John Wiley & Sons; 1982.

Mugnaini E. The length of cerebellar parallel fibers in chicken and rhesus monkey. Journal of Comparative Neurology. 1983; 220(1):7–15. [PubMed: 6643718]

Nicolson GL. The interactions of lectins with animal cell surfaces. International Review of Cytology. 1974 Feb.39:89–190. [PubMed: 4611947]

Orr HT. Cell biology of spinocerebellar ataxia. The Journal of Cell Biology. 2012; 197(2):167–177. [PubMed: 22508507]

Peschanski M, Ralston HJ. Light and electron microscopic evidence of transneuronal labeling with WGA-HRP to trace somatosensory pathways to the thalamus. The Journal of Comparative Neurology. 1985; 236(1):29–41. [PubMed: 3902913]

Quigg M, Elfvin LG, Aidskogius H. Anterograde transynaptic transport of WGA-HRP from spinal afferents to postganglionc symapthetic cells of the stellate ganglion of the guinea pig. Brain Research. 1990; 518:173–178. [PubMed: 1697207]

Reeber SL, Gebre SA, Filatova N, Sillitoe RV. Revealing neural circuit topography in multi-color. Journal of Visualized Experiments: JoVE. 2011a; (57):4–11.

Reeber SL, Gebre S, Sillitoe RV. Fluorescence mapping of afferent topography in three dimensions. Brain Structure & Function. 2011b; 216(3):159–169. [PubMed: 21387082]

Reeber SL, Otis TS, Sillitoe RV. New roles for the cerebellum in health and disease. Frontiers in Systems Neuroscience. 2013 Nov.7:83. [PubMed: 24294192]

Reeber SL, Sillitoe RV. Patterned expression of a cocaine- and amphetamine-regulated transcript peptide reveals complex circuit topography in the rodent cerebellar cortex. The Journal of Comparative Neurology. 2011; 519(9):1781–1796. [PubMed: 21452228]

Ruigrok, TJ., Sillitoe, RV., Voogd, J. The Rat Nervous System. 4th. Academic Press; 2014. Cerebellum and Cerebellar Connections; p. 133-205.

Sakai N, Insolera R, Sillitoe RV, Shi SH, Kaprielian Z. Axon Sorting within the Spinal Cord Marginal Zone via Robo-Mediated Inhibition of N-Cadherin Controls Spinocerebellar Tract Formation. Journal of Neuroscience. 2012; 32(44):15377–15387. [PubMed: 23115176]

Sarna JR, Marzban H, Watanabe M, Hawkes R. Complementary stripes of phospholipase Cbeta3 and Cbeta4 expression by Purkinje cell subsets in the mouse cerebellum. Journal of Comparative Neurology. 2006; 496(3):303–313. [PubMed: 16566000]

Schwab ME, Javoy-Agid F, Agid Y. Labeled wheat germ agglutinin (WGA) as a new, highly sensitive retrograde tracer in the rat brain hippocampal system. Brain Research. 1978; 152(1):145–150. [PubMed: 79432]

Sillitoe RV. Mossy Fibers Terminate Directly Within Purkinje Cell Zones During Mouse Development. Cerebellum. 2016; 15(1):14–17. [PubMed: 26255945]

Sillitoe RV, Vogel MW, Joyner AL. Engrailed homeobox genes regulate establishment of the cerebellar afferent circuit map. Journal of Neuroscience. 2010; 30(30):10015–10024. [PubMed: 20668186]

Sillitoe, RV., Fu, Y., Watson, C. Cerebellum. In: Watson, C.Paxinos, G., Luis, P., editors. The Mouse Nervous System. Elsevier Inc; 2012. p. 360-397.

Sillitoe RV, Hawkes R. Whole-mount immunohistochemistry: a high-throughput screen for patterning defects in the mouse cerebellum. The Journal of Histochemistry and Cytochemistry. 2002; 50(2): 235–244. [PubMed: 11799142]

Staines WA, Kimura H, Fibiger HC, McGeer EG. Peroxidase-labeled lectin as a neuroanatomical tracer: evaluation in a CNS pathway. Brain Research. 1980; 197(2):485–490. [PubMed: 6157452]

Valera AM, Binda F, Pawlowski SA, Dupont J, Rothstein JD, Poulain B, Isope P. Stereotyped spatial patterns of functional synaptic connectivity in the cerebellar cortex. eLife. 2016:1–22.

Van Der Want JJL, Klooster J, Nunes Cardozo B, De Weerd H, Liem RSB. Tract-tracing in the nervous system of vertebrates using horseradish peroxidase and its conjugates: Tracers, chromogens and stabilization for light and electron microscopy. Brain Research Protocols. 1997; 1(3):269–279. [PubMed: 9385065]

Vig J, Goldowitz D, Steindler DA, Eisenman LM. Compartmentation of the reeler cerebellum: Segregation and overlap of spinocerebellar and secondary vestibulocerebellar fibers and their target cells. Neuroscience. 2005; 130(3):735–744. [PubMed: 15590156]

Vogel MW, Prittie J. Topographic Spinocerebellar Mossy Fiber Projections Are Maintained in the Lurcher Mutant. The Journal of Comparative Neurology. 1994; 351:343–341.

Voogd J. What we do not know about cerebellar systems neuroscience. Frontiers in Systems Neuroscience. 2014 Dec.8:227. [PubMed: 25565986]

Voogd J. The importance of fiber connections in the comparative anatomy of the mammalian cerebellum. Neurobiology of Cerebellar Evolution and Development. 1969:493–514.

White JJ, Arancillo M, Stay TL, George-Jones Na, Levy SL, Heck DH, Sillitoe RV. Cerebellar Zonal Patterning Relies on Purkinje Cell Neurotransmission. Journal of Neuroscience. 2014; 34(24): 8231–8245. [PubMed: 24920627]

White JJ, Lin T, Brown AM, Arancillo M, Lackey EP, Stay TL, Sillitoe RV. An optimized surgical approach for obtaining stable extracellular single-unit recordings from the cerebellum of head-fixed behaving mice. Journal of Neuroscience Methods. 2016a; 262:21–31. [PubMed: 26777474]

White JJ, Arancillo M, King A, Lin T, Miterko LN, Gebre SA, Sillitoe RV. Neurobiology of Disease Pathogenesis of severe ataxia and tremor without the typical signs of neurodegeneration. Neurobiology of Disease. 2016b; 86:86–98. [PubMed: 26586559]

White JJ, Sillitoe RV. Development of the cerebellum: from gene expression patterns to circuit maps. *Wiley Interdisciplinary Reviews.* Developmental Biology. 2013; 2(1):149–164. [PubMed: 23799634]

Wilson BK, Hess EJ. Animal models for dystonia. Movement Disorders. 2013; 28(7):982–989. [PubMed: 23893454]

Zaborszky, L.Wouterlood, F., Lanciego, J., editors. Neuroanatomical Tract-Tracing, Molecules, Neurons, and Systems. Springer Verlag; 2010.

Significance Statement

The nervous system is organized into an intricate array of pathways with inter-connected areas. In the brain, these different areas project and receive pathways that are dedicated to specific functions. In order to understand how these tracts and their connections control behaviors such as movement, sensation, and cognition, it is essential to uncover where the axons originate, where they terminate, and the precise trajectories that they take within and between regions. We describe a tract tracing method for marking projections with high resolution. We use the wheat germ agglutinin (WGA) tracer conjugated to Alexa fluorophores to label circuits in multi-color. Using the mouse cerebellum as model, we demonstrate the utility of WGA-Alexa for resolving a wiring diagram that controls movement.

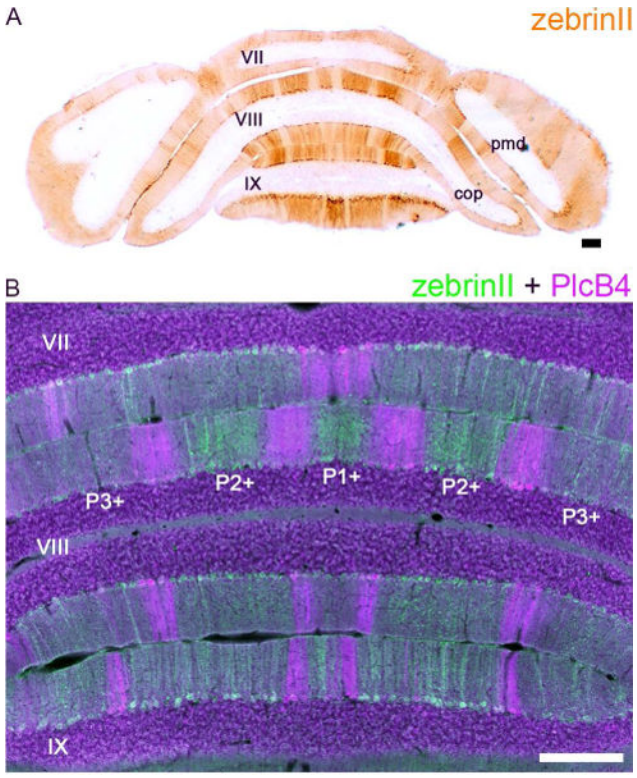

Figure 1.

(A) ZebrinII expression reveals a striking topography of parasagittal zones in the cerebellum. Shown here is a tissue section cut the posterior cerebellum of a control Swiss Webster mouse. **(B)** ZebrinII and PlcB4 are expressed in complementary zones (Sarna et al., 2006). Scale bars = 200 μm. Abbreviations: pmd, paramedian lobule; cop, copula pyramidis. Lobule numbers are indicated by Roman Numerals (Larsell, 1952). The zebrinII positive zones are labeled according to the standard stripe nomenclature (please see Sillitoe and Hawkes, 2002; Apps and Hawkes, 2009).

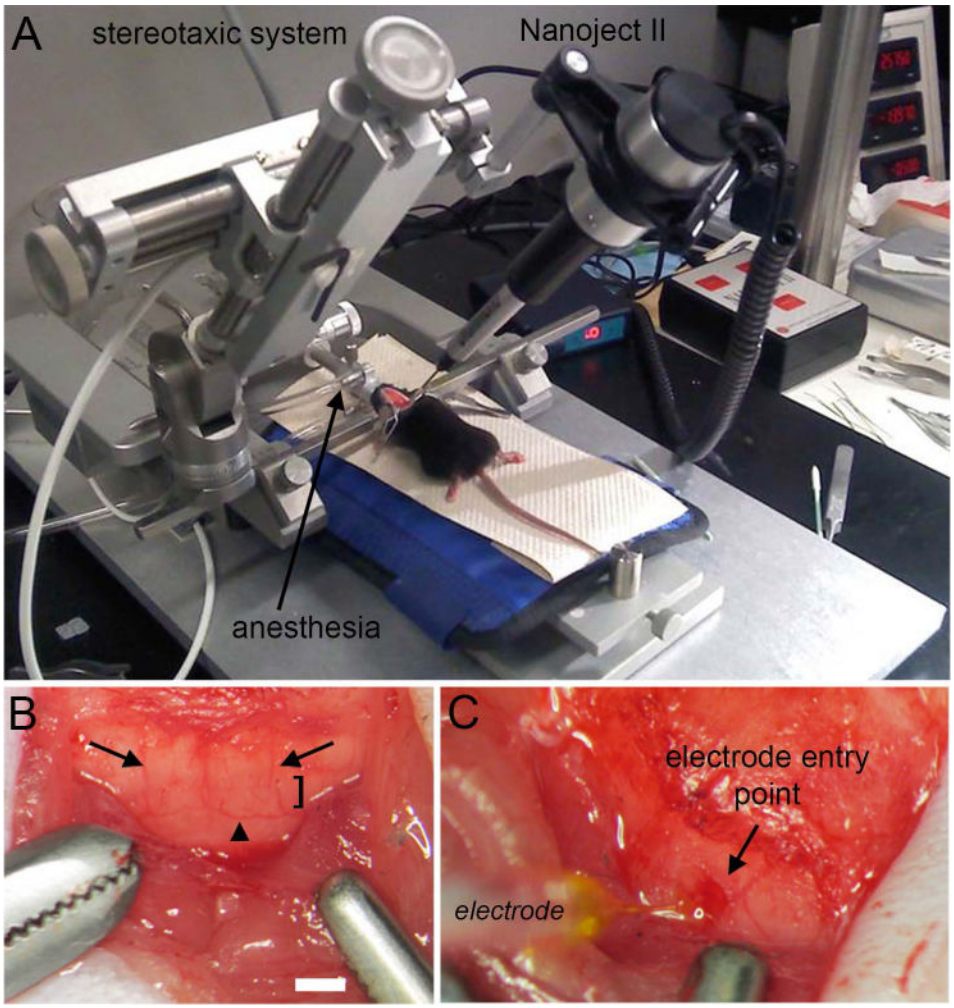

Figure 2.

(A) Surgery and injection set up for using the Nanoject II. **(B)** The posterior cerebellum was exposed during surgery. Lobule VIII is marked with the bracket. Lobule VIII can be identified by its unique saddle shape morphology but also by its vasculature. Dorsomedial cerebellar arteries demarcate the lateral margins of the vermis (arrows), as well as the lower visible aspect of lobule VIII that is adjacent to lobule IX (arrowhead). **(C)** Nanoject II mediated delivery of WGA-Alexa into lobule VIII of the cerebellum. Scale bar in B = 500 μm (= 250 μm in C).

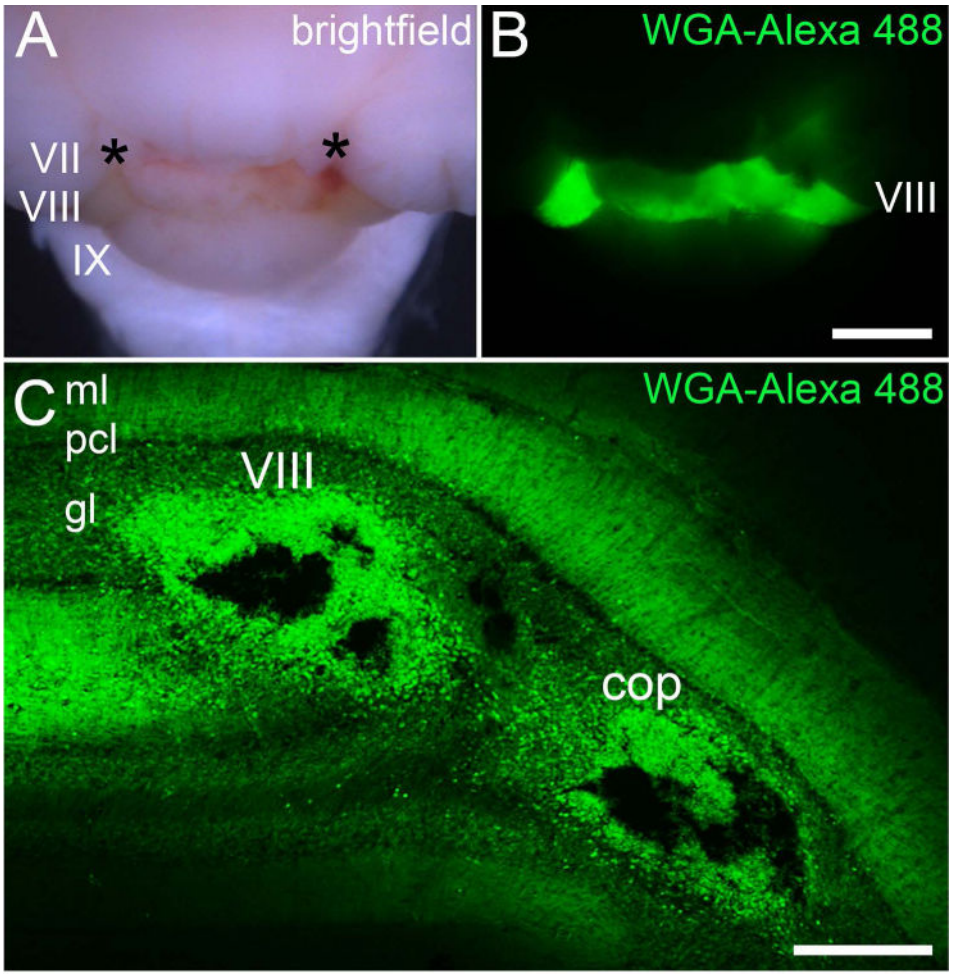

Figure 3.

(A) Brightfield image of the posterior cerebellum after injecting WGA-Alexa 488 into two separate loci (asterisks) in lobule VIII. The light green hue is due to the presence of the Fast Green that was also injected into lobule VIII. **(B)** Fluorescence image showing the spread of WGA-Alexa 488 within lobule VIII. **(C)** Coronal tissue section cut through lobule VIII. Two Nanoject II injections were made, one in the vermis portion of lobule VIII and the other in the hemispheric portion of the lobule, the copula pyramidis. Abbreviations: ml, molecular layer; pcl, Purkinje cell layer; gl, granular layer; cop, copula pyramidis. Lobule numbers are indicated by Roman Numerals (Larsell, 1952). Scale bar = 500 μm in B (applies to A) and 150 μm in C.

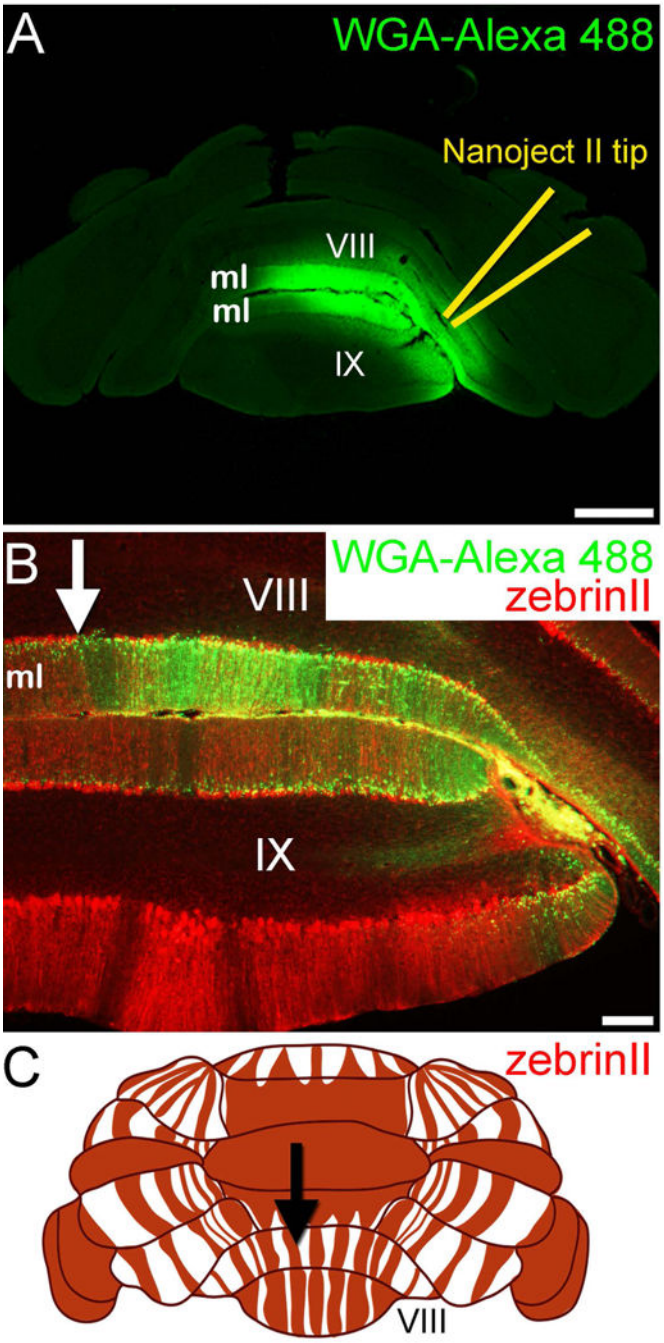

Figure 4.

(A) Nanoject injection of WGA-Alexa 488 into lobule VIII/IX results in dense tracing of the molecular layer (ml) axons. **(B)** The dense staining in the molecular layer is consistent with tracing of granule cell parallel fiber axons. The WGA-Alexa 488 pattern terminates at a zebrinII Purkinje cell boundary (arrow). In this experiment, the mice were given 3-acetylpyridine (3-AP) to remove climbing fiber terminals from the ml, which occurs after the drug kills inferior olive neurons. **(C)** Schematic of the dorsal and posterior cerebellum showing the pattern of zebrinII positive (red) and negative (white) Purkinje cell zones. The

arrow is pointing to the specific zonal boundary that is also marked in panel B. Scale bar in A = 500 μm and 100 μm in B.

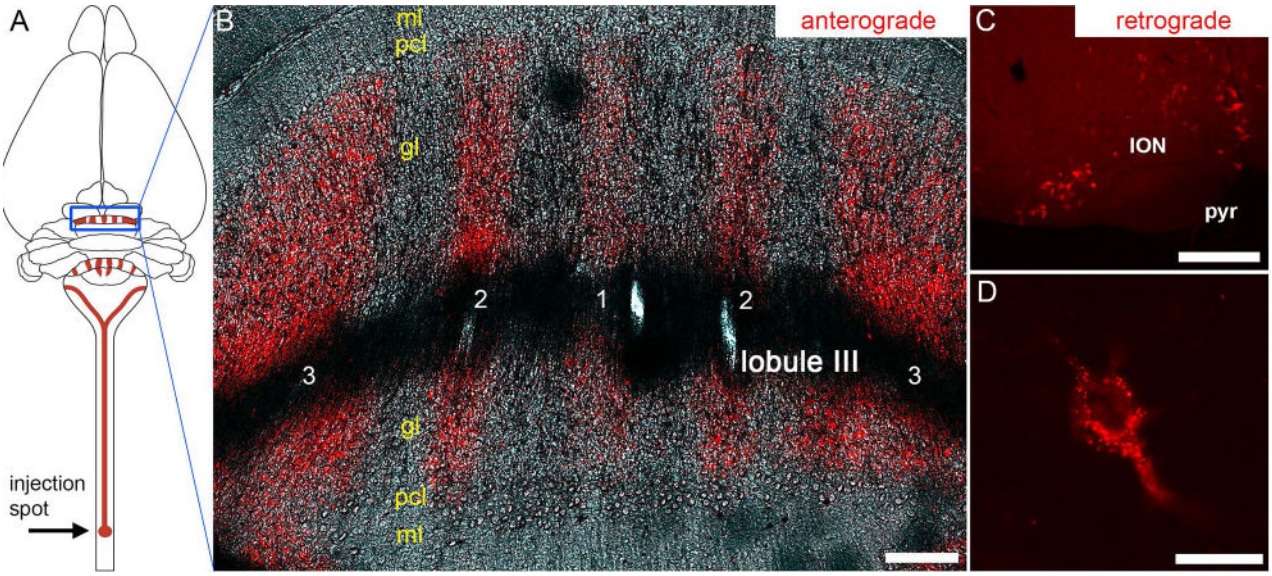

Figure 5.

(A) Schematic illustrating the strategy and overall trajectory and termination pattern of the spinocerebellar tract. The lower thoracic-upper lumbar region was targeted. The blue rectangle outlines the pattern of mossy fiber zones in the anterior cerebellum. **(B)** Coronal tissue section cut through the anterior cerebellum (lobule III) showing the striking pattern of mossy fiber zones after tract tracing with WGA-Alexa 555. The five major zones are labeled as 1-3, with 1 located at the cerebellar midline. **(C)** Injections of WGA-Alexa 555 into the spinal cord also retrogradely trace neurons, and shown here are retrogradely traced somata in the inferior olive. **(D)** Higher power image of a retrogradely traced inferior olive neuron showing the punctate accumulation of WGA-Alexa 555. Abbreviations: ml, molecular layer; pcl, Purkinje cell layer; gl, granular layer; ION, inferior olivary nucleus; pyr, pyramidal tract. Scale bar in B = 150 μm, scale bar in C = 200 μm, and scale bar in D = 20 μm.

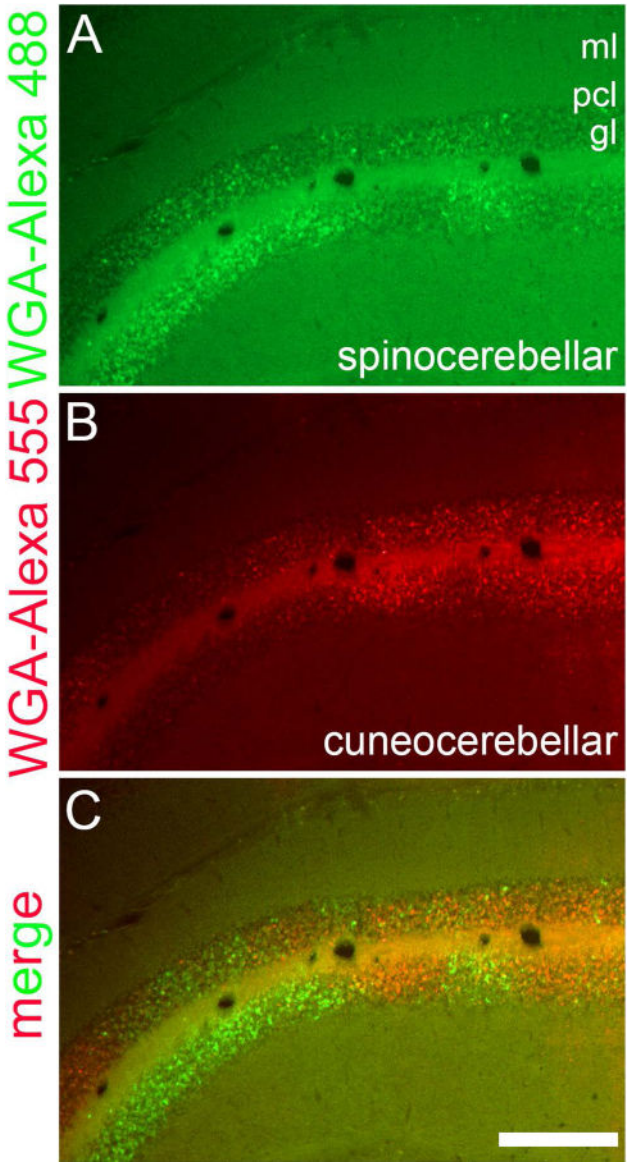

Figure 6.

Coronal tissue section cut through the anterior cerebellum showing the complementary topography of **(A)** spinocerebellar (WGA-Alexa 488) and **(B)** cuneocerebellar (WGA-Alexa 555) mossy fiber domains on one side of the cerebellum. The merged image layers are shown in panel **(C)**. Abbreviations: ml, molecular layer; pcl, Purkinje cell layer; gl, granular layer. Scale bar = 250 μm.

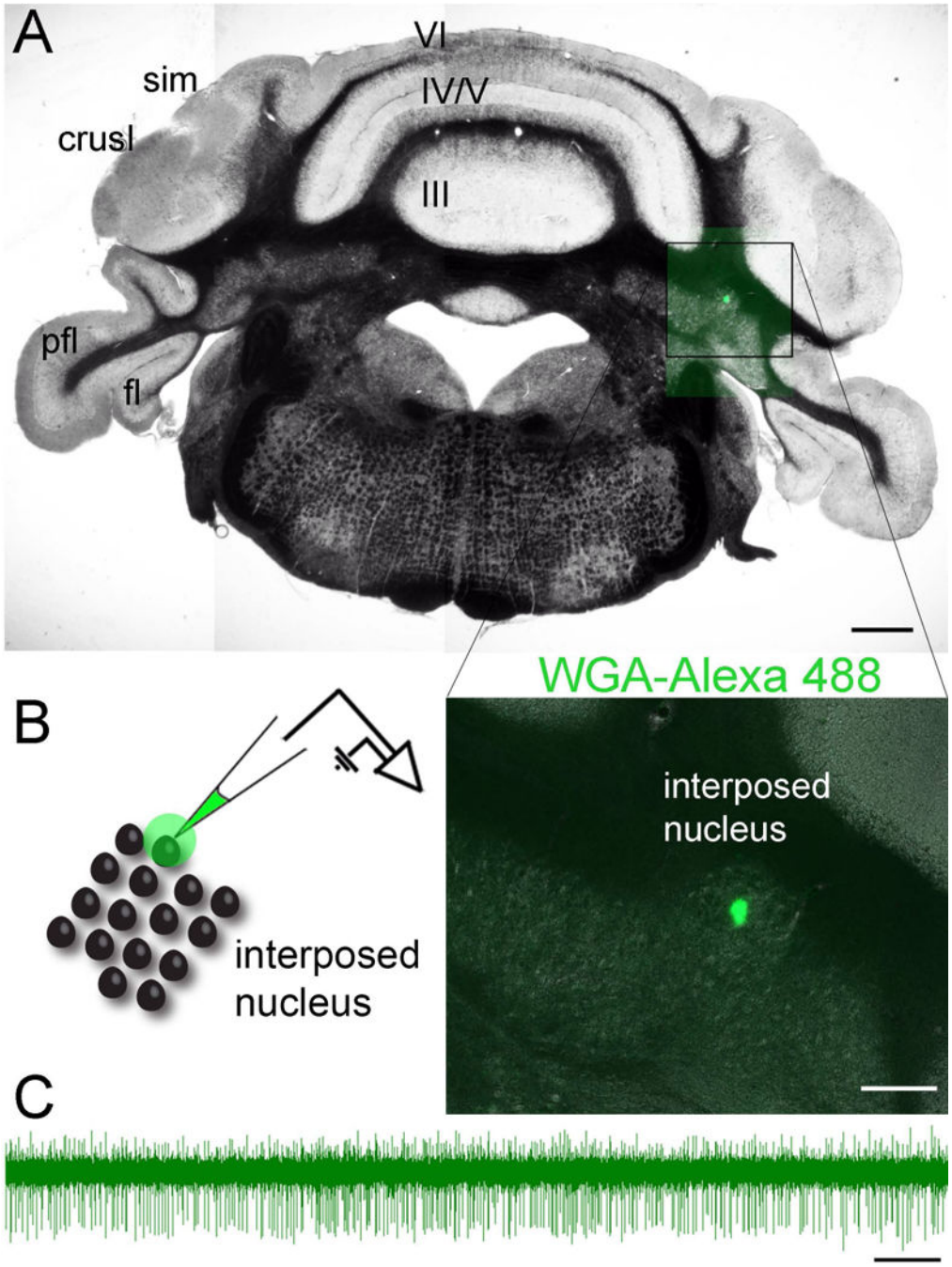

Figure 7.

(A) Coronal tissue section cut through the cerebellum showing the location of cerebellar nuclei neurons that were marked with WGA-Alexa 488 immediately after an *in vivo* electrophysiological recording. **(B)** The schematic on the left shows the strategy for marking and recording a local area within the interposed cerebellar nucleus and the higher power image on the right shows the actual injection spot. **(C)** A sample raw electrophysiology trace from a cerebellar nuclear neuron that was recorded *in vivo* using a glass pipette that was filled with WGA-Alexa 488. Abbreviations (hemisphere lobules): sim, lobules simplex; pfl,

paraflocculus; fl, flocculus. The vermis lobules are indicated by Roman numerals. Scale bar = 500 μm in A, 100 μm in B, and 500 ms in C.